Conventional rotational molding process and aerodynamic characteristics of an axial-flow hollow blades rotor

A. Lucas[1] · A. Danlos[2] · M. Shirinbayan[1,3] · V. Motaharinejad[1] · R. Paridaens[3] · K. Benfriha[4] · F. Bakir[3] · A. Tcharkhtchi[1]

Abstract

In this work, the rotational molding process is developed to manufacture in one piece an axial-flow turbomachine rotor with hollow blades. Giving to our knowledge, this process has never been employed in the making of these turbomachine components. Indeed, the blades of these rotors are typically solid blades and are making by injection molding, machining, or thermoforming. The effects of three relevant factors of the rotational molding process are studied here: oven temperature, time of heating, and cooling rate. The cooling of the moving mold is managed by simple convection-of-air, or by convection-of-air charged with water particles. For the oven temperature of 285 °C, hollow-blades rotors of good quality are gotten in 12 min per cycle. In addition, aerodynamic characteristics of one rotational molded rotor are compared to those of another part machined in aluminum piece. Characteristics of this aluminum rigid-rotor are assumed as reference.

Keywords Rotational molding · Hollow blade · Manufacturing · Axial-flow rotor

1 Introduction

Currently, the rotors are used in various types of turbomachines (pumps, fans, compressors, and turbines). These rotors are categorized giving to the type of flow. When the flow is parallel to the axis of rotation, they are entitled axial-flow rotors. There are many methods for these parts manufacturing like injection molding, machining or thermoforming, and laser forming [1]. Various factors affect the quality of this product during the process. This work looks for to answer the following question: Would it be possible to manufacture by rotational molding an axial-flow fan with aerodynamic characteristics similar to that same turbomachine machined from a rigid material, for example aluminum?

Rotational molding is a process for transforming polymers to hollow parts of broad dimensions, eventually to double-walled [2–7]. The principle of this process is relatively intelligible; however, it allows the manufacturing of complex parts. These two advantages supply the key to its success. The first patent describing a machine like the current rotational molding equipment was filed in 1935 [8]. The introduction of plastisol's (PVC) in 1941 by the company Union Carbide allowed the first developments of rotational molding. The industrial use of polyethylene in 1950 and its availability in

✉ M. Shirinbayan
mohammadali.shirinbayan@ensam.eu

A. Lucas
albert.lucas@ensam.eu

A. Danlos
amelie.danlos@lecnam.net

V. Motaharinejad
vajihe.motaharinejad@ensam.eu

R. Paridaens
richard.paridaens@ensam.eu

K. Benfriha
khaled.benfriha@ensam.eu

F. Bakir
farid.bakir@ensam.eu

A. Tcharkhtchi
abbas.tcharkhtchi@ensam.eu

[1] Arts et Métiers ParisTech, PIMM – UMR CNRS 8006, 151 Boulevard de l'Hôpital, 75013 Paris, France

[2] Le Cnam–DynFluid, 151 Boulevard de l'Hôpital, 75013 Paris, France

[3] Arts et Métiers ParisTech, DynFluid, 151 Boulevard de l'Hôpital, 75013 Paris, France

[4] Arts et Métiers ParisTech, LCPI, 151 Boulevard de l'Hôpital, 75013 Paris, France

micronized form around 1960 will promote this material for this process. There are two types for this process, namely: conventional rotational molding (CRM) that applies the thermoplastic powders without chemical reaction and reactive rotational molding (RRM) that uses reagents (a mixture of monomers or oligomers and chain extenders or hardeners) for polymerization of elastomers and thermosets. However, the CRM is the most common in the industry. Today, only thermoplastic powders exhibiting the characteristics described in [2–5] are used:

Due to restrict of suitable polymers and the lack of published research on CRM or RRM, progresses on these processes have been marginal for a long time. But today, advances in the synthesis of novel polymers and a kinder master of these two processes have helped revive their development. This manufacturing technology is considered today as an alternative to extrusion blow molding.

The novel types of machines, molds, and materials presently available allow the manufacture of high-tech products with sophisticated properties like reinforced polymers or multilayer parts [9–12]. Significant sectors of the market are opening today to rotational molded products. The rotational molding can presently seize its proper place compared to other processes, like extrusion or injection blow molding and thermoforming [13–15].

Axial-flow fans include complex shapes that deliver them specific aerodynamic and acoustic characteristics. The blade thickness stays one factor that affects these properties [16]. Habitually, axial-flow fans allow thin-blades. However, to be able to manufacture the rotor via rotational molding, the thickness of the blades must be relatively larger [16, 17].

The rotational molding process leads to thick and hollow blades. This property of the blades gives the rotor useful advantages which cannot be gained therefore surely by other conventional methods, for example:

- The need to use actuators inserted into the vanes to regulate the flow is satisfied by thicker and hollow blades.
- The blades can be filled with sound absorbing foam.
- An active or passive control by air injection or suction into the clearance gap between the rotating shroud or blades is possible. It is attempted to reduce, respectively, the leakage flow [18] or boundary layers
- We have registered an international patent, which consists chiefly of an axial fan incorporating in the hollow vanes an exchanger where circulates a coolant [19].

The constant quality of technical parts got by rotational molding takes control of the leading material phenomena of the process. However, this control is still perfectible today, because of the sheer number of influence factors. At the PIMM and DynFluid laboratories, we develop a tool for numerical simulation of rotational molding processes [20]. The SPH-solver—Smoothed Particle Hydrodynamics Solver—

incorporates in its physical modeling the results from our experimental work (Fig. 1).

In this paper, an experimental study of an axial-flow fan designed by DynFluid's method [21] and manufactured by conventional rotational molding is presented. The effects of three relevant factors of the process are investigated. In addition, to compare and demonstrate the aerodynamic characteristics of the rotational molded turbomachine, an identical rotor made of aluminum is so manufactured by machining. The two fans only differ in the process of manufacturing. The machined rotor has filled and rigid blades. Conversely, the rotational molded rotor is provided with hollow blades and lightly flexible. The results of these comparisons are explained in Sect. 5.

2 Axial-flow rotor design, procedure of manufacturing, and characterization methods

2.1 Axial-flow rotor design and aerodynamic measurement description

2.1.1 Axial-flow rotor design

The rotor developed in this study is a prototype designed following the method described in reference [21]. Pictures of this, thick blade's rotor are displayed in Fig. 2 with a drawing of a section of the blades at the hub, mid-span, and tip. The main characteristics of the blade cascade are provided in Table 1.

Profile designation NACA 65(xx)yy: (xx) relative camber and yy relative thickness [21].

This rotor allows six blades and is built up from blades with modified NACA-65 profiles, of the mean chord equal to 74 mm. The hub-to-tip ratio is $R_{int}/R_{max} = 0.365$ with tip radius $R_{max} = 179$ mm. The rotor is moreover shrouded with a circular collar. The span wise load of the blades is prescribed following a controlled vortex design method [21]. The blades are stacked on the trailing edge and are swept forward [22]. The maximum blade thickness of the blade is 10 mm, i.e., 13.5% of the chord at mid-span (conventional axial-flow rotors ordinarily have a relative maximum thickness varying from roughly 10% at the hub to 7% at the tip [21]). This axial-flow rotor was designed to meet the specifications point $\Delta p = 230$ Pa, Qvdes (flowrate at design point) $= 0.74$ m^3/s, for an angular velocity $\omega = 262$ rad/s.

2.1.2 Design of mold

The mold is gotten by machining an aluminum block in two parts following to the joint plane of the Fig. 3. Regarding the filling, several solutions are possible. The mode of filling chosen makes it possible to get rotors of good quality and is done by the center and the six blades. It was unnecessary here to complete the filling via the circular collar because the centrifugal effect is

Fig. 1 2D numerical simulation at various times during the rotational molding of a three-blade rotor: four positions around the principal rotation axis [20]
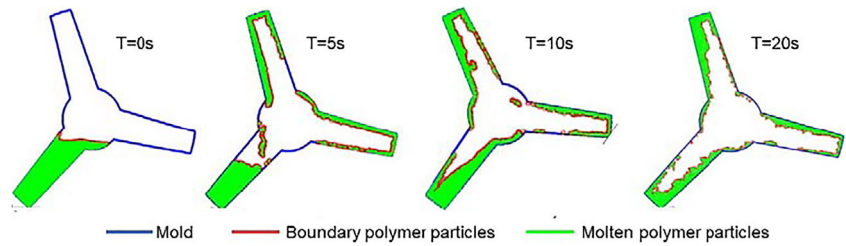
enough to feed the polymer mold at this position. However, it suffers the disadvantage of increasing the mold filling time since it is necessary to unscrew and screw the seven covers (one cap on each blade and one on the hub cover). It is acceptable to compromise at this stage of development, but this filling solution deserves to be rethought for industrialization.

2.1.3 Test bench and aerodynamic measurements

Figure 4 shows the experimental facility used to achieve the global characteristics of axial-flow rotors, in the open-flow configuration. This test benches are designed and built at the DynFluid laboratory following to the ISO-5801 standard. It consists of hexahedron of size $1.3 \times 1.3 \times 1.8$ m³. A pierced plate inside prevents the flow from having prerotation. The axial-flow rotors are placed at one side face. The circular collar being tightly fitted to the bench. The air flowrate is set and measured following to the ISO-5167 standard by setting the hydraulic impedance through diaphragms of various sizes placed at the other side face.

The average static pressure Δp delivered by the rotor is giving using a FCO318 pressure-transmitter model of Furness Controls. This apparatus measures the average pressure between the walls inside the hexahedron and the air ambient, with an accuracy of 0.1 Pa for the range of −999 to +999 Pa. The mass flow rate is directly gotten from the following formula:

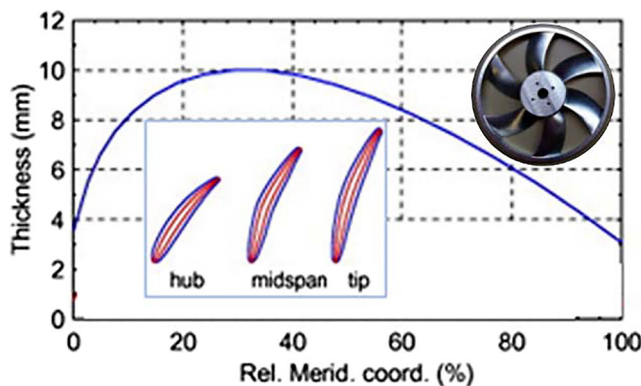$$Q_m = \frac{\alpha \epsilon \pi d^2}{4} \sqrt{2\rho \Delta P} \qquad (1)$$

Fig. 2 Views of the rotor, modified Naca65 profiles at three spans and thickness distribution law along the meridional coordinate

Where:

- d is the diaphragm diameter,
- ΔP is the average static pressure,
- α and ϵ are the constants ($\alpha \epsilon$ H 0.6),
- ρ is the air density.

This mass flow rate is modified, manually, by means of several diaphragms of different diameters placed on the lateral side opposite to that where the rotor is mounted. The torque C on the rotor shaft is read on an HBM strain gauge transducer. The uncertainty corresponds to 0.1% of the maximum measured torque. The angular velocity ω is given by a tachymeter of relative precision ±0.2%. The power adsorbed on the rotor shaft is then estimated via the formula $P = C.\omega$. The combination of these measurements makes to calculate the static efficiency η within about ±0.5% of accuracy ($\eta = \frac{\Delta P.Q_m}{\rho.C.\omega}$).

2.2 Procedure of manufacturing

In this paragraph, the rotational molding machine used and the procedure for getting an axial-flow hollow blade rotor are briefly described. In addition, the influence of three relevant factors of the rotational molding process is mentioned.

2.2.1 Rotational molding machine

The rotational molding machine "LAB 40" (Fig. 5), of Shuttle type built by STP and available in the PIMM laboratory, has employed in this work. This machine is equipped with a computer interface to set its operating factors, namely: the oven temperature, the two rotational speeds and the heating, and cooling times.

2.2.2 Description of used polymer

The material utilized in this study attends a grade of linear low-density polyethylene (LLDPE-3200 natural), supplied by ICO Polymers Company. This polymer has a melt flow index of 3.3 g/10 min (2.16 kg, 190 °C) and a density of 938 kg/m³. LLDPE is sieved to use only 125 to 250-μm particles.

Table 1 Main characteristics of the blade cascade

Layer	Radius (mm)	Chord (mm)	Solidity	Stagger angle (°)	Profile
Hub	65.4	66.6	0.97	53	NACA 65(07)15
Mid-span	122.2	74.0	0.58	66	NACA 65(10)13,5
Tip	179.0	81.3	0.43	70	NACA 65(11)12

2.2.3 Description of the rotational molding procedure

At the beginning, the required amount of 500 g powder-polyethylene is introduced into the mold's cavity (Fig. 6). This mold is then closed and is placed in the oven. During the heating phase, the mold slowly rotates on two axes (3.3 rpm and 7.1 rpm). The heat transfer melts the polymer powder. This molten material practically uniformly plasters all the inner walls of the mold. The temperature of the molten polymer reached is well greater than the value of its temperature at the melting point.

In the second step, the mold is moved to the cooling station. It is alternatively chilled using blown air followed by a water spray. Clearly, rapid cooling is desirable for economic reasons, but this can cause problems like warping. In the ultimate step, the rotation is stopped, and the mold is outputted from the machine. Ultimately, the mold is opened, and the manufactured part is de-molded. Another cycle is so then ready for beginning.

2.2.4 Choice of some factors of the process

When the oven temperature is not high enough, the time necessary rising to the melting point (T_m) of the polymer becomes important. In this case, if the time adopted for a cycle is through, so then the material will be completely unmelted and which causes malformations in molded part: moderate strength, stiffness, and ductility. Conversely, if the polymer overheats at a temperature above the melting point, degradation will occur and the piece will represent insufficient quality. For better controlling the temperature of the polymer or internal mold air over time, the most effective way is to operate the equipment that tracks the temperature. In fact, by recording this factor, it is possible to observe the changes in the state of the material during the process in real time. In this case, the rotational molded part is of good quality (devoid of a problem of degradation).

It is in addition noticed that the method of cooling the mold, following the heating phase, can cause a significant effect on the quality of the part.

The values of the three factors selected in this study for the rotational molding process are

- Two oven temperatures: 285 and 330 °C
- Two heating times: 12 and 20 min.
- Two cooling rates: (i) by blown air only or (ii) by blown air coupled with a water spray

2.3 Characterization methods

To better follow the rotational molding process of the developed rotor, different characterization methods were used:

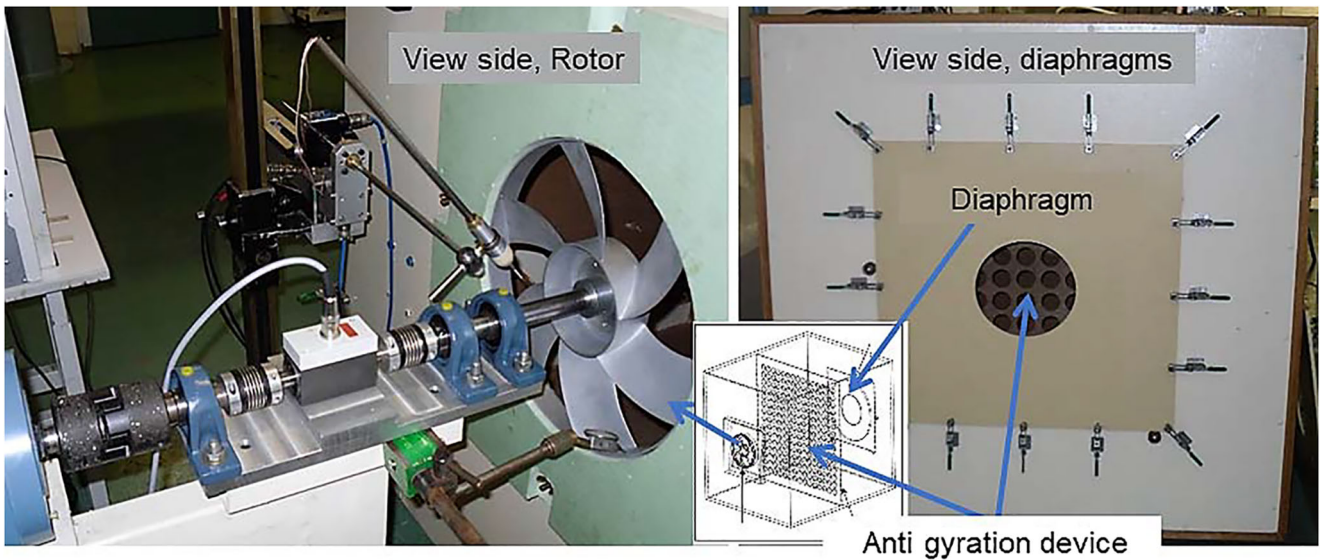**Fig. 3** Used mold for produced polyethylene rotor by rotational molding

Fig. 4 ISO-5801 test bench: side views, rotor, and diaphragm

2.3.1 Thickness measurement

To control the material thickness of rotors after the rotational molding process, eight positions are chosen to collect specimens, including one in each pressure side of the six blades. Figure 7 illustrates these eight points. Thickness values are measured using a precision micrometer "0–25 mm/ 0.001 mm (AK9635D)". Rotational molding process conditions affect the average material thickness. However, that when these conditions are the same, no significant difference is observed between the thicknesses of the specimens taken. The repeatability of the process seems to be checked.

2.3.2 Fourier transform infrared spectroscopy

FTIR spectrometry (IR Spotlight 300), in reflection mode, is used to inspect the part after manufacturing and to be sure that there is no oxidation during the process. In fact, the polymer is sensitive to oxygen for the elevated temperatures especially all along with the rotational molding. The cycle time of this process is relatively long, and in the absence of pressure and mechanical loading, the temperature is persistently high. Therefore, the risk of thermal degradation is not negligible.
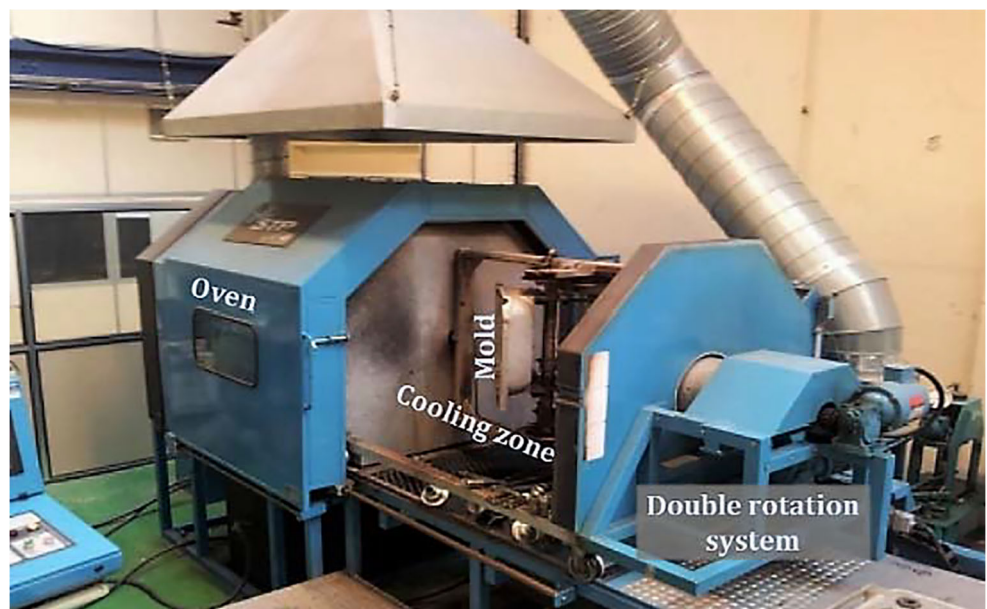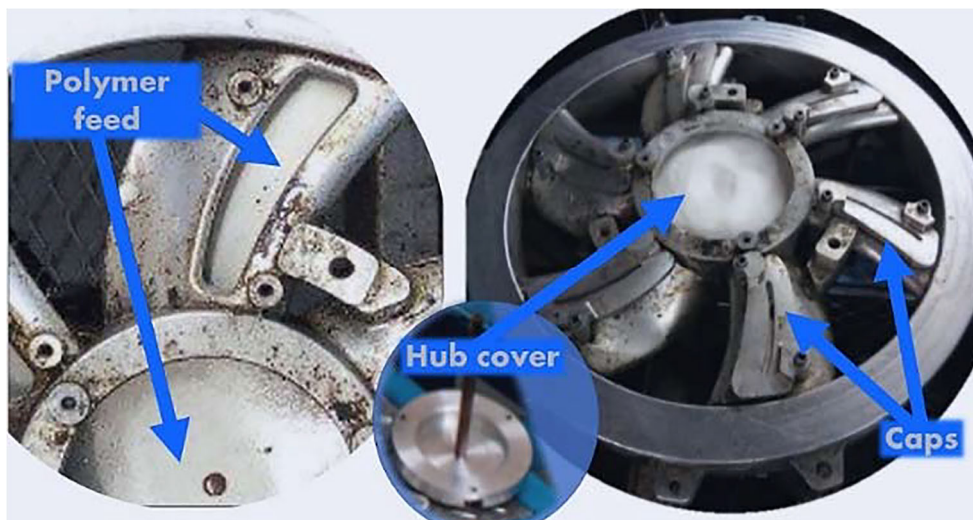
Fig. 5 Rotational molding machine LAB 40

Fig. 6 LLDPE filling channels of the mold

2.3.3 Differential scanning calorimetry test

The melting and crystallization temperatures (T_m and T_C) of the polyethylene chosen are determined by thermal analysis employing a device of the "TA Instruments Q10 DSC" type. Specimens of 6.75 mg mass are acquired from the rotational molded parts. These specimens are placed in hermetic aluminum capsules. To eliminate the effect of the thermal history of the material, each specimen is first heated to 180 °C with a velocity of 2 °C/min, then cooled to room-temperature around 25 °C with the same speed. After this initial phase, these specimens are heated again, at a heating rate of 2 °C/min, to a temperature above the melting point of the polymer. This second phase makes it possible to determine the graphs giving the temperatures T_m and T_C as well as the degree of crystallinity.

2.3.4 Thermo-mechanical analysis

To measure the main transition temperatures like α transition (related to the glass transition temperature), dynamic-mechanical-thermal analysis (DMTA) tests have performed on parallelepiped specimens, using "DMA Q800" instrument, from TA Company. The tests have been realized at the following condition: alternating bending configuration, temperature range from 30 to 100 °C, frequency 1 Hz, and temperature rates 2 °C/min.

2.3.5 Quasi-static tensile tests

Tensile tests were performed with an "INSTRON 5966" machine at room temperature. The strain rate was 2 mm/min. Dog bone shape specimens with gauge length and width equal to 10 mm and 2 mm, respectively, were employed.

2.3.6 SEM observations

Microscopic observations, using scanning electronic microscope "HITACHI 4800 SEM", have performed in the aim qualitatively to investigate the material microstructure.

3 Results and discussions

3.1 Evolution of the polymer during the rotational molding cycle

During a thermal cycle in this process, the material passes from solid state to liquid state, to match the shapes of the mold, then inversely from liquid to solid state to congeal the final shapes of the part. Experimentally, it is possible to place the thermocouples at diverse locations to measure the changes in temperature.

As before mentioned, two oven temperatures, 285 and 330 °C, two heating times, 12 and 20 min, and two cooling rates, by only blown-air and by blown-air coupled with a water-spray, were chosen to assess the effect of these three factors in the rotational molding process. Finally, four

Fig. 7 Thickness measurement locations

manufacturing A, B, C, and D modes were chosen (Table 2). An identical amount of PE powder (500 g) is utilized in each of four cases. The macroscopic images, the masses, and the average thicknesses, gotten for each rotor, are presented.

Figure 8 represents the evolution of the temperature during the different steps of the process for A, B, C, and D modes, with the periods of heating and cooling. This figure also illustrates the behavior of the polyethylene in the mold as well as on its phase changes. These diagrams allow monitoring of the changes in the physical state of polyethylene and make it possible to distinguish several stages during the process. For example, for the A condition:

- From the beginning of the curve to point I, the mold temperature increases to reach a temperature close to the melting temperature of the material (≈ 120 °C in the case of a semi-crystalline polyethylene).
- At the point I, the first layer of polymer grains in contact with the internal surface of the mold reaches the melting polyethylene temperature, and because of sintering phenomenon (coalescence and densification), it is transformed into a first molten layer on the inner surface of the aluminum mold. This phenomenon is en continually repeated, and for each rotation cycle, a new molten layer is formed on the previous layer. The layers of the material begin arranging one after the other. In this way, the thickness of part is formed between points II and I.
- Between points II and III, the molten polymer increasingly becomes fluid. Therefore, the diffusion and migration of air bubbles are easier. Therefore, the trapped air between the grains will be extracted from the molten material thanks to densification.
- Between III and IV, the mold is placed in the cooling station, and so, the temperature of the polymer decreases.
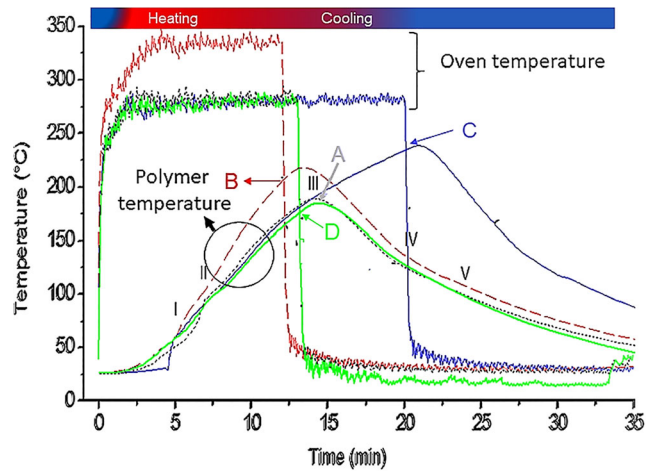

Fig. 8 Temperature evolution of oven and polymer during rotational molding process

However, the material is continually staying at a liquid state. The last air bubbles may be extracted in this period.
- Point IV corresponds to the crystallization temperature of polyethylene. At this temperature, the polymer begins to be solidified. Between IV and V, a liquid-solid mixture is present. Beyond V, the material is completely solidified, and the piece is formed.

3.2 Multiscale characterizations of the rotational molded parts

3.2.1 Thickness measurement

Thickness measurements of pieces produced showed uniform rotor could be gained with the four modes. Nevertheless,

Table 2 Macroscopic images, masses, and the average thicknesses of the molded rotors

Part name	A	B	C	D
Oven Temperature	285 °C	330 °C	285°C	285°C
Oven Time	12 min	12 min	20 min	12 min
Cooling mode	Air	Air	Air	Air and Water
Macroscopic images				
Masses	500 (g)	500 (g)	486 (g)	500 (g)
Average thicknesses	2.03 (mm)	1.91 (mm)	1.85 (mm)	**2.03** mm)

macroscopic images show that the color of the piece produced by the A mode is less clear. To check this change of color depends on the light oxidations during rotational molding, FTIR tests have been performed on the specimens make.

3.2.2 Infrared analysis

The evolution of [C=O] concentration provides a precise description of the oxidation process and the degree of degradation in the polymer. One can indicate the location of the peaks at the wave numbers of 1780 cm^{-1}, 1735 cm^{-1}, and 1710 cm^{-1}.

Figure 9 shows the IR spectra of polyethylene made by the four modes. From these results, it seems that any C=O groups are formed during the process due to oxidation. However, the sensitivity of this method is limited and cannot reveal the consumption of the stabilizer and the formation of the deep concentration of chemical groups. It is then necessary to investigate this subject in more details.

3.2.3 DSC analysis

Figure 10 presents the DSC measurement results for the four modes. These curves show the same melting and crystallization temperatures for the pieces produced by A and D modes: 125 and 115 °C successively. Likewise, for the pieces produced by B and C modes. These two temperatures are successively 128 and 118 °C. The melting and crystallization temperatures of the pieces produced by B and C modes are higher. This increase of melting point may be related to the fact that the crystalline morphology of the specimen produced by these modes is more thermostable. If this hypothesis is accurate, then we can suppose that the crystallinity is raised. In fact, we observe in the amorphous phase of the oxidation and the chains scission, and the rearrangement of macromolecules and their orientation. The increase in crystallinity makes the polymer more thermostable.
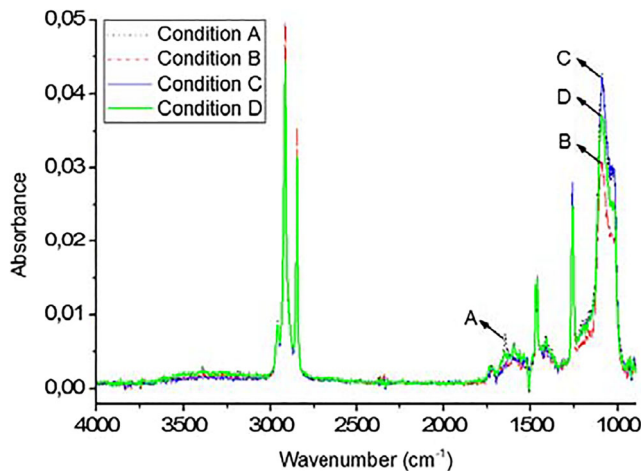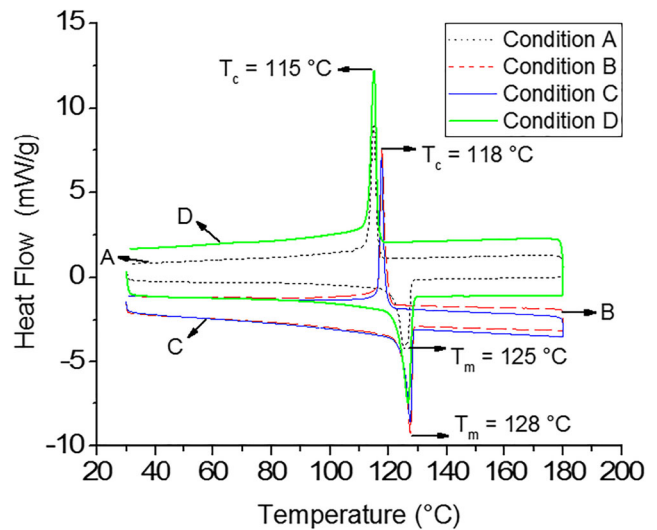
Fig. 10 DSC results of A, B, C, and D modes

3.2.4 Tensile behavior

The results after eight tensile tests at room-temperature for the rotors presented in Fig. 11 indicated the similar tensile behavior of specimens, at various zones of each rotor. This confirms the stability of the properties of the tensile. Tensile test results clarify the influence of aging on the mechanical properties of polyethylene. Oxidation leads to the loss of ductility and the increase of resistance and stiffness. One can observe the decrease of failure strain in the case of the specimen by B and C modes. In the case of B mode, this decrease of ductility can be explained by the fact that as the oven temperature is higher; 330 °C, the polymer-temperature is higher too, because of the oxidation and chain scission, the polymer becomes more brittle. In the same way because of the growth of crystallinity (even perhaps because of cross-linking), its stiffness and its resistance increase. The value of Young's modulus of the
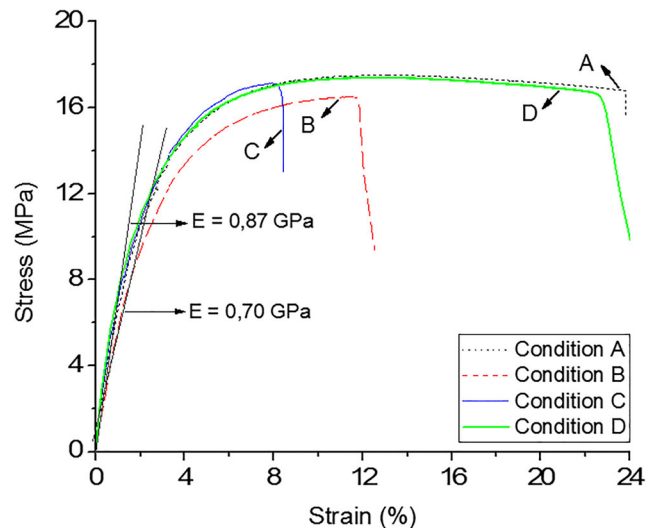
Fig. 9 IR spectrum of pieces obtained by the A, B, C, and D modes

Fig. 11 Quasi-static tensile behavior at room temperature

specimen resulted in A mode is about 0.7 GPa which is lower than those of the specimen produced by B mode: 0.87 GPa. The failure stresses demonstrate the similar tendency for the four cases.

3.2.5 Thermo-mechanical properties

DMTA test is preferentially performed to study the transitions' temperatures T_α, T_β, T_γ and changes of state of polymers. To compare the specimens resulted by the four modes, DMTA-tests are performed with the alternating bending configuration and in the temperature range between 30 and 100 °C. In these experiments, the amorphous phase of polyethylene is in the rubbery state. The molecular mobility in this state is superior, and the polymer is subtle. There are globally all transitions in this range. However, the results of the tests (Fig. 12) show that there is only one transition around 50 °C. The literature indicates that for some semi-crystalline polymers, there is a transition called this "TαC transition", in the temperature range between T_g and T_c. This one is related to the mobility of the macromolecular segments of the amorphous phase which are near or in connection to the crystalline lamellas. In the case of polyethylene utilized, it may be logically assumed that this significant change around 50 °C, of the E′and E″, is related to this "TαC transition".

Figure 12 illustrates that E′ related to the B condition is a little higher than E′ in A condition for the same reason as explained before for the results of quasi-static mechanical tests. Moreover, one can note that there is no difference of thermo-mechanical properties for A and C modes.

3.2.6 Crystalline morphology

The cooling-rate can influence the properties of the finished piece like morphology of materials. In the case of semi-crystalline polymers, this factor causes more effect on the crystallization phenomenon and the rate of spherulites growth and their size. However, some of the semi-crystalline polymers, like
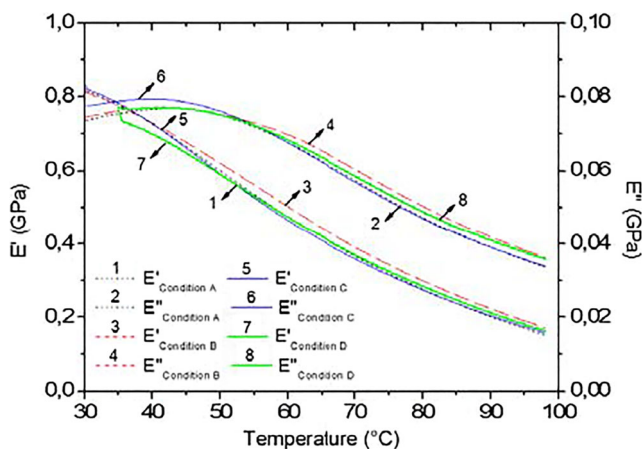

Fig. 12 DMTA scan of A, B, C, and D modes

polyethylene, maintain a relatively elevated crystallization rate. In this case, the effect of the cooling rate is less significant. Figure 13 shows that there is no significant difference in the crystalline morphology of the two A and D modes corresponding, as mentioned above, to two types of cooling rate.

4 Process results discussion

4.1 Effect of oven temperature

Temperature is one of the significant factors during the rotational molding process. In Sect. 3.1, more details about the evolution of this factor are expressed. As the pieces produced by condition A have practically been unoxidized, the heating temperature of 285 °C is proposed for oven temperature.

4.2 Effect of cycle time

Another factor that has an effect on the quality of the piece is the heating (curing) time. If the heating time is short, a part of powder is not enough time to be transformed and the piece cannot be completely manufactured. Conversely, if this time is elevated, there is a risk of degradation (oxidation).

Oxidation of the polymer may produce the hydroperoxide, which can vary the color of the piece especially the color of its internal surface.

Two heating times, 12 and 20 min, were chosen to assess the effect of oven time at a selected oven temperature: 285 °C and cooling by air. Macroscopic image of the piece produced by the C condition clearly displayed the yellowish color of the product. In addition, the tensile test results showed more failure stress in the case of oven time of 20 min. As a result, the oven time of 12 min is proposed.

4.3 Influence of cooling rate

Many studies showed that the method of cooling could cause a significant effect on the quality of the product. The mechanical properties of the plastic will be rather various in each method. The most critical issue is that, in the rotational molding, cooling is from the outside of the mold only. The drop of the cooling rate and this asymmetric configuration results in warping and distortion of the molded part. Slower cooling tends to improve the strength and stiffness of the plastic but reduces its resistance to impact loading. Fast-cooling reduces time-molding but the piece manufactured is less stiff. The shape and dimensions of the part equally will be affected by the cooling rate.

After many tests, the cooling rate is managed here via two modes, the A mode, convection of exclusive air around the moving mold. The D mode, jet of water-spray, is included.

However, for these two modes, no significant difference is observed in the analysis methods: infrared, DSC, tensile
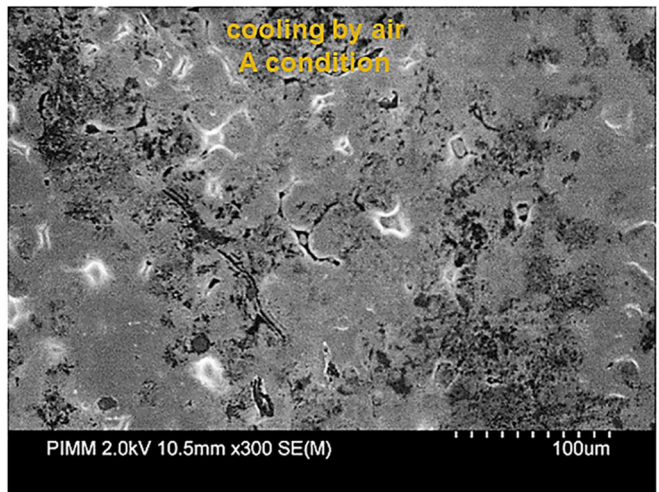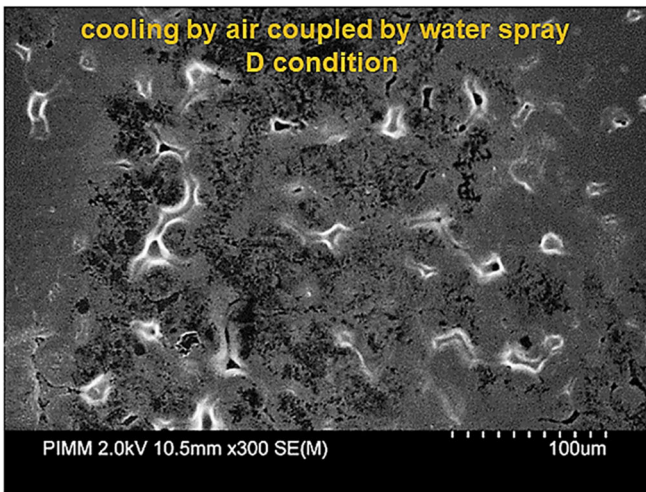
Fig. 13 Crystalline morphology: cooling by air coupled by water-spray (left), cooling by air (right)

behavior, thermomechanical properties, and crystalline morphology.

However, it can be noticed that industrial companies in the field of rotational molding process prefer the cooling by air, because it is an economical method.

5 Global characteristics of axial-flow rotors

As already mentioned, to compare global characteristics of the rotor made by aluminum with that of rotational molded rotor

of the condition A (Fig. 14), an experimental study is performed.

These two machines have the same geometric data and shapes, except that the molded rotor possesses hollow blades. It is therefore more likely to deform during rotation and so, perhaps change his aerodynamics characteristics.

5.1 Aerodynamic characteristics

The aerodynamic characteristics of these two rotors were measured on the test bench described above. These characteristics:

Fig. 14 An aluminum axial flow rotor (left) and polymer rotor (right)
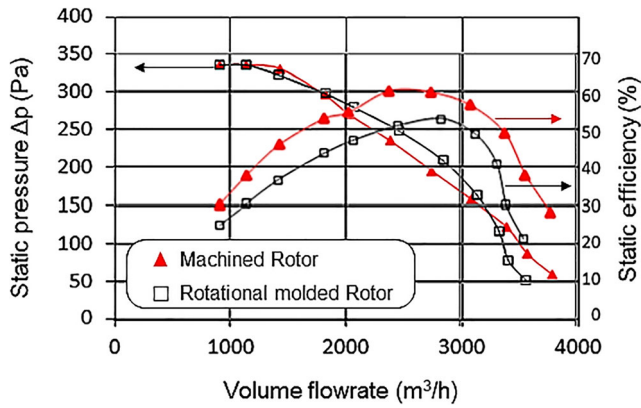
Fig. 15 Rotor characteristics at 2500 rpm: static pressure and static efficiency vs. volume flow rate

Fig. 16 Square amplitude spectra of wall pressure fluctuations at of volume flow rate, Qv = 0.442 m³/s and 1500 rpm. Machined rotor (black), rotational molded rotor (red)

the static pressure and static efficiency versus flow rate are shown in Fig. 15. Apart from the drop of efficiency of the polymer rotor, the other characteristics values and tendencies are fairly similar.

5.2 Pressure fluctuations

The measurements of the pressure fluctuations at the wall casing of the two rotors' shroud were performed at ω = 157.08 rad s⁻¹ (1500 rpm) during 10 s corresponding broadly to 250 rotor rotations and sampled at 12 kHz. The ducted flow facility of DynFluid, presented in reference [23], is used. The recorded signals were treated, with MATLAB, using the modified welch-average Fourier transform. The spectra S(f) is expressed in dB following the formula:

$$S(f) = 20\log_{10}\left(\frac{p'(f)}{p_{ref}}\right) \qquad (2)$$

The wall pressure fluctuations are investigated at of homologous design volume flow rate, Qv = 0.442 m³/s. The corresponding spectra are displayed in Fig. 16, at 1500 rpm. The two rotors exhibit relatively notable discrete peaks, corresponding to blade passing frequency at f_{bpf} (150 Hz) and its harmonics. The level of the fundamental for the polymer rotor is 10.9 dB and its first harmonic reach 3.2 dB and the second harmonic − 14.5 dB. The spectrum of the aluminum rotor shows the fundamental and the four-first harmonics. The fundamental harmonic reaches no more than 5.0 dB.

Then again, the two rotors show in their spectra a peak at f = 24.9 Hz. This frequency corresponds to the rotation frequency (1500 RPM/60 s). This harmonic could have till six harmonics, depending on the signals recorded. This frequency indicates either the rotor is mounted unbalanced or the deformation creates a dynamic unbalance generating this frequency. Peaks values are higher for hollow blades rotor than the machined rotor. This increase could be explained by a stronger dynamic unbalance on this rotor because of its deformation.
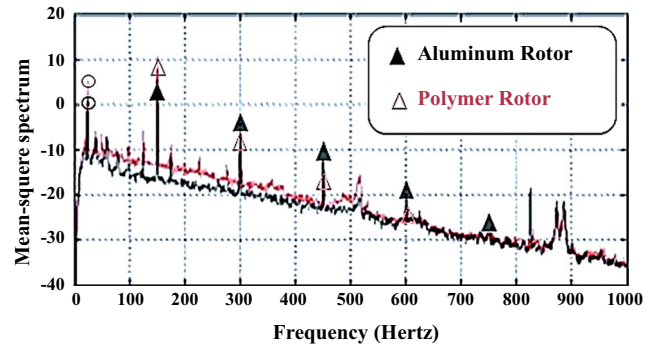
From this first study and as a preliminary conclusion, the rotational molded rotor shows promising capabilities. Some points must be improved, namely making the rotor more rigid by adopting another material, conceivable with the rotational molded process. It would also be effective to inspect the deformation with high-speed imaging.

6 Conclusion

In this work, the fulfillment of the rotational molding process for the manufacture of an axial flow rotor has been presented. The temperature, the time-heating, and the cooling mode are the significant factors during the rotational molding process that effect on the quality of the piece. If the heating time is too short, a part of powder has not enough time to be transformed and the piece cannot be completely transformed. If it is too high, there is a risk of degradation (oxidation). One can notice that oxidation of the polymer may produce the hydroperoxide that change the color of the piece especially the color of its internal surface. After different analysis like physical-chemical characterization, tensile behavior, and thermomechanical properties of rotational molded rotors, the chosen process conditions are finally summarized below:

- The oven temperature is equal 285 °C.
- The baking time is equal 12 min.
- The cooling rate is managed by simple convection of air around the moving mold (between 1 and 2 °C per minute).

The aerodynamic characteristics comparison between the aluminum and rotational molded rotors showed that the static efficiency is lower for the rotational molded rotor.

The wall pressure fluctuations are also investigated at of design volume flow rate. The power spectral density (PSD) level at the fundamental harmonic is higher for the hollow blade's rotor. This is likely justified to the poor balance of this rotor and its relative flexibility. As evidenced by the noise it generates, and, the drop of static efficiency observed.

Solutions that provide more rigidity to the blades should be tested shortly. Despite these disadvantages of the rotational molded rotor, the results are promising.

In the future, to minimize the material cost used in this process, blends of virgin LLDPE with other materials will be investigated like for example recycled HDPE [24]. Various ratios of blending, to consider the morphology, mechanical properties, and the relation of melt flow rate and rheology will be implemented.

In the long term, after the optimization of the process, we hope that the rotational molding will be used especially for large axial flow rotor sizes and small series.

References

1. Xiang R, Zhou J, Xiong Y, Liu J, Wang H (2017) Hot forming of complex surface of hollow blade back arc based on drawing process. Int J Adv Manuf Technol 93(9–12):4015–4021
2. Crawford RJ, Gibson S (2006) Rotational molding: the basics for designers. Rotoworld, pp 60–66
3. Tcharkhtchi A, Verdu J (2004) Structure-processability relationships during rotational moulding of plastics. Adv Eng Mater 6(12):983–992
4. Crawford R (1996) Rotational moulding of plastics. Polym Eng Ser New York Res Stud Press
5. Zonszain I (1998) Rotomoulage peu connu mais performant. Plast Mod élastomères 50(9):36–39
6. Oliveira M, Cramez J (2001) Rotational molding of polyolefins: processing, morphology, and properties. J Macromol Sci Part B 40(3–4):457–471
7. Hafsaoui SL, Benziane M, Tcharkhtchi A (2013) Thermal transfer simulation regarding the rotational moulding of polyamide 11. J Therm Anal Calorim 112(1):285–292
8. Ferngren ET, Kopitke WH (1939) Apparatus for forming hollow articles from organic plastic material. 3
9. Iwakura K, Ohta Y, Chen CH, White JL (2017) Experimental investigation of rotational molding and the characterization of rotationally molded polyethylene-parts. Inten Polym Process IV 91:399–404
10. Throne JL (1972) Some factors influencing cooling rates of rotationally molded parts. Polym Eng Sci 12(5):335–339
11. Tcharkhtchi A, Briot J, Crawford RG, Robert A, Kearn M (2001) Rotomoulage du polyéthylène chargé mica. Mater Tech 89:37–43 2011
12. Tcharkhtchi A, Barcelo P, Mazabraud P, Jousse F, Kearns MP (2002) Study of adhesion between two layers in multilayer rotomolded products. Adv Eng Mater 4(7):475–478
13. Narkis M, Puterman M, Boneh H, Kenig S (1982) Rotational molding of thermosetting three-phase syntactic foams. Polym Eng Sci 22(7):417–421
14. Tcharkhtchi A (2005) Mechanism of foaming during rotational molding. Int J Form Process 8(4):363–382
15. Liu SJ, Tsai CH (1999) An experimental study of foamed polyethylene in rotational molding. Polym Eng Sci 39(9):1776–1786
16. Sarraf C, Nouri H, Ravelet F, Bakir F (2011) Experimental study of blade thickness effects on the overall and local characteristics of a controlled vortex designed axial-flow fan. Exp Thermal Fluid Sci 35(4):684–693
17. Marrero MD, Hernández P, Suárez L, Pestana D, Benítez A, Martín J, Rivero S, Calero E (2014) Rotational molding applied to the manufacturing of blades of small wind turbine. ASME 2014 12th Bienn Conf Eng Syst Des Anal 3
18. Azzam T, Paridaens R, Ravelet F, Khelladi S, Oualli H, Bakir F (2017) Experimental investigation of an actively controlled automotive cooling fan using steady air injection in the leakage gap. Proc Inst Mech Eng Part A J Power Energy 231(1):59–67
19. Azzouz K, Khelladi S, and Bakir F (2017) Motor-fan assembly comprising a hydraulic heat transfer fluid cooling circuit. Pub. No. WO/2017/149227, Int Appl
20. Hamidi A, Khelladi S, Illoul L, Shirinbayan M, Bakir F, Tcharkhtchi A (2015) Modelling surface tension with smoothed particle hydrodynamics in reactive rotational moulding. Comput Fluids 118:191–203
21. Noguera SKR, Rey R, Massouh F, and Bakir F (1993) Design and analysis of axial pumps. ASME Fluids Eng Second Pump Mach Symp Washington, USA, pp 95–111
22. Hurault J, Kouidri S, Bakir F, Rey R (2010) Experimental and numerical study of the sweep effect on three-dimensional flow downstream of axial flow fans. Flow Meas Instrum 21(2):155–165
23. Nouri H, Ravelet F, Sarraf C, and Bakir F (2010) Experimental study of blade rigidity effects on the global and the local performances of a thick blades axial-flow fan. ASME, p FEDSM-ICNMM2010-30623
24. Chaisrichawla S, Dangtungee R (2018) The usage of recycled material in rotational molding process for production of septic tank. Mater Sci Forum 936:151–158